Dendrochronologia 85 (2024) 126197

Contents lists available at ScienceDirect

Dendrochronologia

journal homepage: www.elsevier.com/locate/dendro

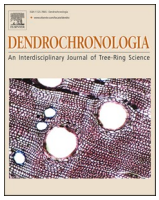

Pine processionary moth outbreaks and droughts have different tree ring signatures in Mediterranean pines

Hermine Houdas [a,*], José Miguel Olano [a], Héctor Hernández-Alonso [a], Cristina Gómez [a,b], Miguel García-Hidalgo [a], Darío Domingo [a,c], Antonio Delgado-Huertas [d], Gabriel Sangüesa-Barreda [a]

[a] iuFOR, EiFAB, Universidad de Valladolid, Soria, Spain
[b] Department of Geography and Environment, University of Aberdeen, UK
[c] GEOFOREST-IUCA, Departamento de Geografía, Universidad de Zaragoza / Spain
[d] Instituto Andaluz de Ciencias de la Tierra, IACT, (CSIC-UGR), Spain

ARTICLE INFO

Keywords:
blue intensity
drought
insect defoliations
latewood
stable isotopes
tree growth

ABSTRACT

Defoliating insects' outbreaks play a critical role in trees' carbon cycle. The pine processionary moth (PPM; *Thaumetopoea pityocampa*) is the major defoliating insect of Mediterranean coniferous forests. The frequency and intensity of PPM outbreaks is projected to increase as winter temperatures become milder due to climate warming. An accurate evaluation of this projection requires a wide spatial baseline of the historical PPM incidence. PPM outbreaks affect tree secondary growth leading to narrow rings, providing a tree level signal. However, PPM defoliation rings can be confounded with drought rings, the most frequent cause of narrow rings in Mediterranean environments. Thus, an accurate identification of PPM rings demands the consideration of additional tree ring traits. Here, we introduce a multiproxy approach to identify and distinguish PPM and drought events. We sampled four *Pinus nigra* (3) and *P. sylvestris* (1) stands in Spain. We identified and verified years of PPM defoliation using remote sensing analysis and field observations of Regional Forest Service. We identified drought events through the combination of climatic data with radial growth reductions. We considered climate growth residuals, among-trees growth variability, latewood percentage (%LW), intrinsic water-use efficiency (iWUE) and minimum blue intensity (BI) to discern between droughts and PPM outbreaks. In comparison with drought rings, PPM rings showed 1) more negative residuals in climate growth models, 2) higher secondary growth variance, 3) higher percentage of latewood and 4) lower iWUE. Minimum BI did not differ between drought and PPM rings, but was lower than in the rest of the rings. The combination of these traits provides a signature to identify PPM rings, opening the opportunity to reconstruct PPM incidence on a broad spatio-temporal scale.

1. Introduction

Forests cover nearly a third of emerged lands and hold more than double the current amount of carbon in the atmosphere (FAO, 2005; Field and Raupach, 2004). Yet, their carbon-fixing capacity is limited by disturbances such as wildfires and insect outbreaks (Dale et al., 2000; Ramsfield et al., 2016). Insect outbreaks reduce tree growth, induce widespread tree mortality, and alter plant dynamics and nutrient cycling (Dymond et al., 2010; Field and Raupach, 2004; Kurz et al., 2008). Integrating outbreak dynamics into carbon cycle models is imperative to ascertain the evolution of climate change over time (Pan et al., 2011; Volney and Fleming, 2000).

Ectothermic organisms, such as overwintering insects, exhibit high sensitivity to temperature fluctuations (Ayres and Lombardero, 2000; Wilson and Fox, 2021). In fact, ongoing temperature rise has been linked to both a higher frequency and intensity of insect outbreaks (Netherer and Schopf, 2010; Robinet and Roques, 2010). In seasonal ecosystems, the increase in winter temperature plays a pivotal role as low temperatures severely constrain the development and survival of insects, consequently limiting insect population sizes (Harrington et al., 2001)

Abbreviations: %LW, latewood percentage; BAI, basal area increment; BI, blue intensity; iWUE, intrinsic water-use efficiency; PPM, pine processionary moth.

* Corresponding author.
E-mail address: herminejosephine.houdas@uva.es (H. Houdas).

https://doi.org/10.1016/j.dendro.2024.126197
Received 17 November 2023; Received in revised form 27 February 2024; Accepted 16 March 2024
Available online 20 March 2024

and distribution ranges (Démolin, 1969).

The pine processionary moth (PPM, *Thaumetopoea pityocampa* Denis and Schiffermüller) is the main defoliating insect of pine and cedar forests in the Mediterranean Basin (Roques et al., 2015). The larvae of this univoltine species feed on needles in winter, leading to individual defoliation rate of up to 100% of crown volume (Jacquet et al., 2012). Despite the predictions of PPM altitudinal and latitudinal spread due to current global warming (Battisti et al., 2005; Battisti et al., 2006; Buffo et al., 2007), we still need long-term data of outbreak dynamics to contextualize potential and current changes. Indeed, research on PPM population dynamics primarily relies on field observations (Azcárate et al., 2023, Hódar et al., 2012). Thus, existing records rarely span more than two or three decades, and longer-term data are typically restricted to specific areas (e.g., Gazol et al., 2019). These datasets hold significant value, but their spatio-temporal perspective is insufficient to contextualize long-term population changes as those attributed to global change, especially considering that PPM outbreaks occur on average every 9–14 years (Camarero et al., 2022). Remote sensing offers a promising avenue for monitoring insect-induced defoliation patterns, including PPM (Otsu et al., 2018; Sangüesa-Barreda et al., 2014), thanks to its frequent revisit time (e.g., 8 days with Landsat, 5 days with Sentinel-2) and its extensive spatial coverage on data collection (Senf et al., 2017). Nevertheless, its temporal depth is limited to mid-term temporal scales (up to 50 years). In addition to stand records provided by field observations and remote sensing data, it is imperative to evaluate tree-scale response to PPM defoliations. We need to understand the defoliation effects on tree physiology to interpret defoliation cascading impacts on the ecosystems affecting carbon, nitrogen and water fluxes, and altering plant-plant and plant-animal interactions (Laurent et al., 2017).

Dendrochronology has been employed to reconstruct defoliation outbreaks at tree level (Esper et al., 2007). Defoliations are usually associated to sharp decreases in secondary growth. However, in temperate ecosystems, droughts also result in high-frequency growth reductions (Camarero et al., 2013; Lucas-Borja et al., 2021) which potentially lead to confounding patterns. Different approaches have been adopted to discriminate these signals. Disparities in annual radial growth patterns between host trees and individuals from non-host species growing in the same ecological conditions have been used to distinguish PPM defoliations from climate-driven signatures (Lynch, 2012). Nevertheless, as the response to drought at different time scales is also species-specific (Pasho et al., 2011), this method may lead to inaccurate interpretations. Particularly, since PPM feeds on most pine species (Barbaro and Battisti, 2011), the comparison of the growth of host trees with coexisting species from different genera and families like *Juniperus* and *Quercus* reduces the validity of such an approach. Alternatively, the growth synchrony of host trees could help to discern between both disturbances. PPM events usually affect trees within a stand to varying degrees, with a higher incidence at the stand's edge (Azcárate et al., 2023). In contrast, droughts tend to reduce tree growth throughout stands, prevailing growth synchrony (Sangüesa-Barreda et al., 2019; Shestakova et al., 2016).

Analyzing additional wood traits (e.g., percentage of latewood within rings, stable isotopes or microdensity) may contribute to improve our ability to discriminate PPM defoliations from droughts. The percentage of earlywood and latewood in tree rings after PPM defoliation could change in comparison to drought as PPM defoliation alters carbon availability for wood lignification (Jacquet et al., 2012; Palacio et al., 2012), leaving a distinctive record in intra-annual wood rates. For another perspective, insect defoliations have been related to ^{13}C-enriched wood (Simard et al., 2008), although another study of one PPM event indicated the presence of ^{13}C-depleted wood after defoliation (Camarero et al., 2023), posing potential on this trait. Finally, wood density has a most solid support with maximum wood density being a good proxy for reconstructing defoliation events, such as larch budmoth outbreaks (Esper et al., 2007; Kunz et al., 2023). The biological rationale behind this signal is also robust, pointing a limited carbon availability (Briffa et al., 2002; Olano et al., 2012). However, little is known about the impact of PPM on wood microdensity, except that minimum density no longer responds to climate in the year following defoliation (Camarero et al., 2023).

Here, our objectives were: (1) to identify changes in tree ring traits as proxies of PPM incidence at tree level in different pine species (*Pinus nigra* and *P. sylvestris*); and (2) to develop a multi-proxy framework for delineating PPM-induced defoliations from the impact of drought. We hypothesized that PPM defoliations lead to (i) a lower growth synchrony because PPM variably affects trees within a stand, resulting in non-uniform impacts; (ii) narrow rings, which could not be explained by climate, corresponding to negative residuals in climate growth models; (iii) a higher percentage of latewood within rings, since PPM defoliations mainly affect earlywood formation; (iv) a lower iWUE due to a reduced water stress induced by higher sapwood canopy ratios; and (v) a decrease in maximum density compared to drought years because trees allocate non-structural carbohydrates towards the production of new leaves, inducing consequently a resource depletion during latewood formation.

2. Material and methods

2.1. Study areas and sampling design

We sampled four forest stands in Spain comprising two pine species vulnerable to PPM defoliations: *Pinus nigra* and *P. sylvestris* (Fig. 1). Among these stands, three were of *Pinus nigra*, recognized as the most palatable species with the highest PPM defoliation levels (Camarero et al., 2022; Hódar et al., 2002; Stastny et al., 2006). All sampled forest stands were monospecific plantations, and according to data from the Regional Forest Service, they have experienced severe PPM-induced defoliations in the past two decades. In each stand, we sampled a total of thirty individuals, following a transect from the edge to the inner parts of the stand.

We extracted three cores from each tree using 5.15 mm diameter Pressler increment borers. Two cores were used for tree ring width chronologies and blue intensity (BI) measurements, while the third core was used for carbon isotope analyses. We recorded the position of individuals employing a submetric GPS receiver (Trimble Geo 7X), and we measured tree diameter at breast height (DBH) (Table 1). Wood cores were stored in straws with an identifier and transferred to the laboratory for processing. Finally, we calculated the distance between each individual tree and the forest edge using high resolution orthophoto mosaics (PNOA, National Program for Aerial Orthophoto) in QGIS 3.26 software (QGIS Development Team, 2023), except for Caltojar and Bayubas stands, characterized by their sparse forest structure and the absence of forest edge effect.

2.2. Identification and verification of PPM defoliation events using remote sensing

To identify PPM events, we explored Landsat-derived normalized difference vegetation index (NDVI) time series spanning from 1990 to 2020. NDVI dense time series are widely recognized as a proxy for primary productivity (e.g., Goward and Dye, 1987; Vicente-Serrano et al., 2016). Albeit drought can also cause NDVI reductions in pine species (Gazol et al., 2023), dense NDVI time series point to PPM events when an NDVI anomaly starts in winter. To build NDVI dense time series corresponding to our stand locations, we retrieved all high-quality observations available on the Google Earth Engine (GEE) cloud platform. We interpolated missing values with a third order polynomial to ensure the construction of a consistent 7-day series. Additionally, we extracted seasonal series corresponding with winter, spring, summer and autumn periods from the comprehensive dataset to explore annual trends at various times of the year. To identify the presence of anomalies associated with a reduction in NDVI during winter, we employed the

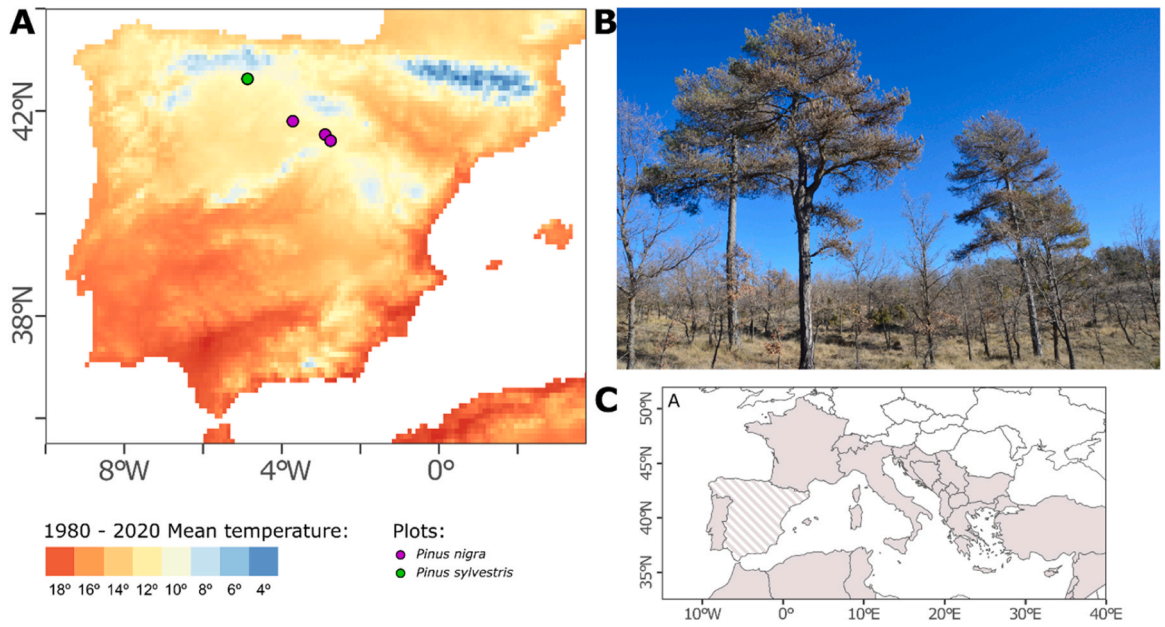

Fig. 1. A) Location of the study areas. Purple and green points represent *Pinus nigra* and *P. sylvestris* stands, respectively. The mean temperature of the 1980–2020 period is also represented. B) Intense pine processionary moth (PPM) defoliation on *Pinus nigra* trees during winter 2021–2022. C) Spatial distribution of PPM. The stripes situate Peninsular Spain in Europe, and the grey fill indicates countries where PPM presence has been reported (Kriticos et al., 2013).

Table 1
Main features of each forest stand: species, latitude (ºN), longitude (ºW), elevation in m.a.s.l, diameter at breast height (DBH) in cm, tree ring series time span, tree age in years and ring width in mm of the sampled trees (mean ± standard error).

Stand	Species	Lat	Long	Elevation	DBH	Time span	Age	Ring width
Bayubas	*P. nigra*	41.54	-2.90	958	18.4 ± 3.0	1974–2021	39.6 ± 0.7	1.8 ± 0.06
Caltojar	*P. nigra*	41.42	-2.76	1040	19.7 ± 3.5	1964–2021	45.9 ± 1.2	1.5 ± 0.08
Oquillas	*P. nigra*	41.80	-3.72	938	27.6 ± 0.7	1961–2021	52.9 ± 1.4	2.0 ± 0.09
Saldaña	*P. sylvestris*	42.58	-4.87	1013	26.4 ± 0.7	1977–2021	36.6 ± 0.8	2.8 ± 0.10

bfastmonitor algorithm (Verbesselt et al., 2010) which marks the timing and magnitude of anomalies. Moreover, we used forest monitoring information from Castilla y León Regional Forest Service to verify the dates of PPM defoliations.

2.3. Tree ring width and basal area increment chronologies

Two cores were mounted on standard wooden supports and fine sanded. They were digitalized using CaptuRING, a semi-automatic camera system (Nikon D7500 with a Tokina Macro 100 F2.8 lens) connected to a computer which allows the acquisition of high-resolution images (≈ 3.7–4.5 μm per pixel; García-Hidalgo et al., 2022). Images were merged with PTGui (New House Internet Services BV, Netherland). Tree rings were measured and crossdated with CooRecorder (Cybis Elektronik and Data AB, Sweden). Crossdating quality was checked using the COFECHA program (Holmes, 1983) (Cybis Elektronik and Data AB, Sweden). Additionally, we discerned earlywood (EW) and latewood (LW) in ten selected trees by assessing sudden changes in the ring pattern. These measurements were used to extract EW width and LW width to calculate latewood percentage (%LW) at ring level.

Annual tree ring width series were transformed into basal area increments (BAI) and averaged per tree. BAI is a more biologically meaningful variable to quantify radial growth trends and changes than tree ring width, being less affected by tree allometry and becoming stable at tree maturity (Biondi and Qeadan, 2008). As the sampled trees were relatively young (maximum 44–60 years old at the end of 2020), we prevented from the positive trend during the juvenile phase by fitting a smoothing spline, with a 50% frequency cut-off set at 2/3 of series length, to all BAI raw series. Both BAI values calculations and detrending were run using the functions *bai.out* and *detrend* from the *dplR* package (Bunn, 2008) in R environment (R Core Team, 2023), respectively. Then, we constructed detrended BAI index chronologies at tree level, and we calculated the growth variance, that is, the variance in the BAI index values for each year and stand.

2.4. Climatic data

We used CRU high-resolution gridded datasets of the 1901–2020 period (Harris et al., 2020; https://crudata.uea.ac.uk/cru/data/hrg/) to obtain monthly mean data of mean temperature, maximum temperature, minimum temperature and precipitation for each forest stand. Additionally, to analyze the effect of drought severity, we calculated the Standardized Precipitation-Evapotranspiration Index (SPEI) for the study period. SPEI is a standardized multiscale drought index based on water balance. Negative and positive values correspond to dry and wet periods, respectively (Vicente-Serrano et al., 2010). We calculated SPEI with monthly resolution using a lag comprised from one to twelve months. For each forest stand, we identified the SPEI timing and lag with the highest correlation with BAI.

2.5. Identification of drought events

We identified dry years as those with SPEI values below –0.5, which is considered a threshold for drought (Wang et al., 2021). In addition to climate data, we focused on the drought impact, and we calculated if these years corresponded to negative pointer years in the tree ring width chronologies (i.e., extremely narrow rings) using the relative growth change approach (Schweingruber et al., 1990). We defined negative

pointer years as those with at least a 30% reduction in BAI compared to the average of the 2 previous years, and when this growth reduction was present in at least 60% of trees in each stand. Drought events were assigned to the years fulfilling these two conditions. For this analysis, we used the *pointer.rgc* function of the *pointRes* R package (Van der Maaten-Theunissen et al., 2015).

2.6. Climate growth models

We modelled BAI response to SPEI to distinguish growth reductions attributable to drought from those due to PPM outbreaks using linear mixed models (LMMs). We hypothesized that residuals will be more negative during PPM events. Our models included the SPEI with maximum signal for the considered period as fixed factor, and previous year BAI and tree as random factors to consider the first-order temporal autocorrelation and to incorporate the non-independent structure of our data, respectively. A separate model was conducted for each stand for the 1990–2020 period and fitted using Restricted Maximum Likelihood (REML). Residuals normality and homoscedasticity were checked to confirm the assumptions of LMMs. In the case of violations of these assumptions, models were re-fitted considering different variance structures (Zuur et al., 2009). Residuals were extracted from the models for every tree and year for further analyses. We used the R package *nlme* (Pinheiro et al., 2023) to fit LMMs.

2.7. Intrinsic water-use efficiency

To assess changes in annual iWUE, we evaluated $^{13}C/^{12}C$ isotope ratio for each site in the 1990–2020 period. We selected five individuals per study site with a narrow tree ring during PPM events and extracted the resin from the cores through a pentane bath for 72 hours before air-drying (Polge, 1970). Each annual ring from 1990 to 2020 was identified and separated with a scalpel. Then, tree rings corresponding to the same calendar year were merged and grounded using a ball mill (Retsch MM400, Retsch GmbH). The samples were weighed, packed in tin caps and combusted at 1000°C in an elemental analyzer (NA1500 series 2, Carlo Erba Instruments). Gas chromatography was used to extract CO_2, which was then transported by a current of helium to an interface connected to an isotope ratio mass spectrometer (Deltaplus XP, Thermo Electron). Analyses were carried out in the Andalusian Earth Science Institute (IACT) in Granada (Spain). Through this technique, we calculated $\delta^{13}C$ of our samples, expressed as the relative difference between the ratio $^{13}C/^{12}C$ (parts per thousand, ‰) and the standard V-PDB. These measurements were used to calculate isotopic discrimination (Δ; Farquhar and Richards, 1984; McCarroll and Loader, 2004), which was then converted to the iWUE (expressed in μmol of CO_2 per mole of H_2O), using available data of $\delta^{13}C$ in atmospheric CO_2 (Graven et al., 2017) and atmospheric CO_2 concentrations. To understand how iWUE varies over time, we calculated iWUE temporal changes as the value of each year relative to the two previous years. This transformation was also applied to BAI data to allow the contrast between both variables.

2.8. Blue intensity

We used BI technique as a proxy of maximum microdensity (Kaczka et al., 2018; McCarroll et al., 2002). We selected ten trees per stand, among those showing response to PPM events. Resin from the cores was extracted using a pentane bath for 72 hours before being air-dried (Polge, 1970). Cores were then mounted on wooden supports and photographed using CaptuRING, with strict incident light control under a dark box, and using the GretagMacbeth ColorChecker® card for colour standardization (García-Hidalgo et al., 2023).

BI was measured with ρ-MtreeRing (García-Hidalgo et al., 2021). As BI is inversely correlated with density (Rydval et al., 2014), we adjusted the light calibration curve to allow direct comparison between BI and wood density. Image resolution was ≈5800 dpi. We analyzed BI by setting a 50 pixels wide path to prevent from wood or processing artefacts (e.g., cracks, discoloration, empty resin ducts) during density profile extraction. Finally, we extracted minimum BI values at ring level, that is, maximum values in density profiles, as a proxy of maximum wood microdensity.

2.9. Statistical analyses

We assessed the potential of the different proxies (growth variance, climate growth model residuals, iWUE temporal changes and minimum BI) to discriminate between PPM and drought events through LMMs. Models included the whole data set (4 stands) and had the same fixed structure (event type as a binomial parameter 1 for PPM and 0 for drought) as well as a random component, either tree nested in stand for parameters measured at tree level (climate growth model residuals, minimum BI) or stand for data measured at yearly level (growth variance and iWUE temporal changes). To analyze %LW, we fitted generalized linear mixed models (GLMMs) with a binomial family, treating the type of event (PPM/drought) as a fixed factor, and accounting for tree nested within year. We checked normality and homoscedasticity of the residuals, proceeding to refit the models with different variance structures whenever these assumptions were not met (Zuur et al., 2009). LMMs and GLMMs were fitted using the R package *nlme* (Pinheiro et al., 2023).

3. Results

3.1. Identification of PPM and drought events

Remote sensing analyses helped identify five years with PPM events during the 1990–2020 period. Each stand showed one or two PPM events (Table A.1). PPM defoliations exhibited a particular spectral signature, with a significant drop in seasonal NDVI values between winter and spring, which was not observed on other years. The *bfastmonitor* algorithm also flagged anomalies in NDVI intra-annual curves (Fig. A.1). Furthermore, the most recent events matched the information reported by Castilla y Léon Regional Forest Service. We also identified between four and seven drought events per stand, in nine different years, which did not coincide with PPM events. Drought events in 2005 and 2012 were common to all stands, while 2002 drought was observed in three out of four stands (Table A.1).

3.2. Basal area increment chronologies

BAI index showed lower values during PPM (mean ± SE, 0.55 ± 0.04) and drought (0.58 ± 0.01) events in comparison with the rest of the years (1.10 ± 0.01). Trees responded synchronically to drought events, whereas secondary growth during PPM events had a higher variance, with trees showing drastic reductions coexisting with trees without growth reductions (Fig. 2), except for Oquillas stand. LMM reflected this asynchrony with higher BAI index variance during PPM events ($P = 0.023$) (Table 2; Table A.2).

3.3. Climate growth models

BAI of Bayubas stand was significantly influenced by April SPEI with an 8-month lag. Similarly, BAI in Caltojar was notably influenced by July SPEI with an 11-month lag, while BAI in Oquillas was driven by May SPEI with the same 11-month lag. In Saldaña stand, BAI responded to January SPEI with a 5-month lag. Pearson's correlations values ranged from 0.28 to 0.52 (Table A.1), the lowest value corresponded to the *P. sylvestris* stand.

PPM events had lower residuals (-0.50 ± 0.04) in the climate growth models than drought events (-0.20 ± 0.01) (Fig. 3). Accordingly, the climate growth model residuals showed significant differences between PPM and drought events ($P < 0.001$; Table 2; Table A.3). Interestingly,

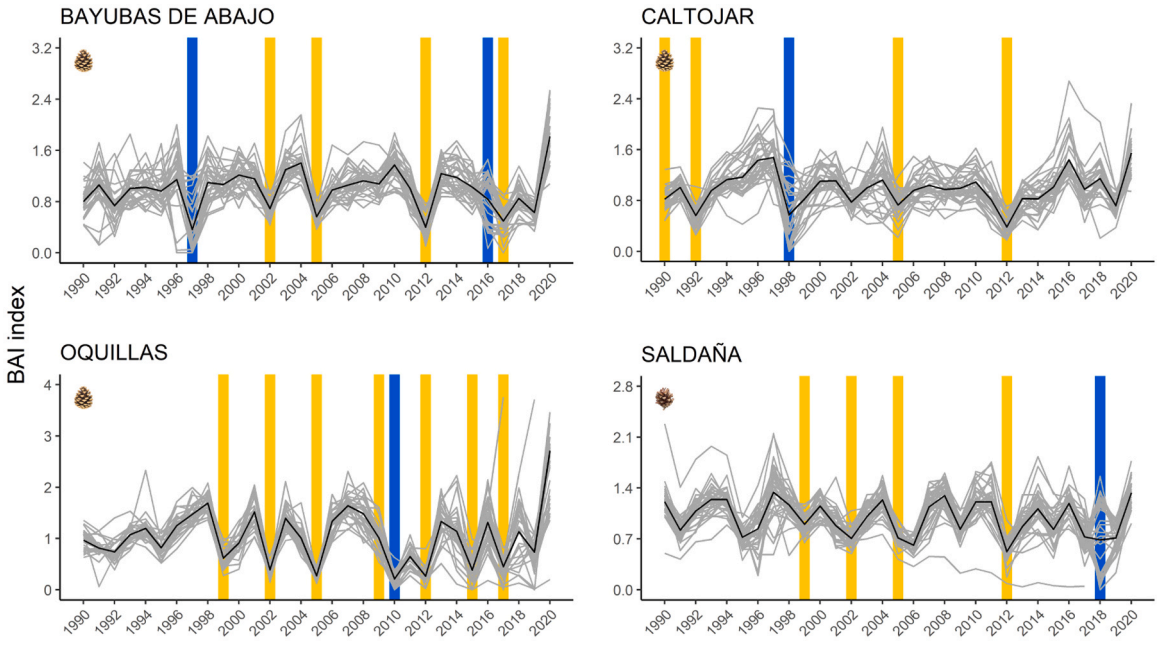

Fig. 2. Variation of detrended basal area increment (BAI) for Bayubas (*P. nigra*; n=34), Caltojar (*P. nigra;* n=32), Oquillas (*P. nigra;* n=29) and Saldaña (*P. sylvestris*; n=37) stands over the period 1990–2020. PPM events and droughts are highlighted in blue and yellow, respectively. The black lines represent the mean detrended BAI.

Table 2
Results of the performed linear mixed models (LMMs) for assessing the differences between PPM and drought events considering: growth variance, climate growth residuals, percentage of LW (%LW), intrinsic water-use efficiency (iWUE) temporal changes, and minimum blue intensity (BI). The sign of the relationship indicates whether PPM events had positive or negative impact compared to drought events. Values in the two last columns indicate the marginal (fixed factors alone) and conditional (fixed and random factors) pseudo-R^2 values.

	PPM events	*P*	Marginal R^2	Conditional R^2
Growth variance	+	0.023	0.210	0.210
Climate growth residuals	-	<0.001	0.133	0.155
%LW	+	<0.001	0.304	0.304
iWUE temporal changes	-	<0.001	0.437	0.633
Minimum BI	n.s	0.882	0.000	0.561

trees located at the forest edge exhibited the lowest residuals in PPM events (Fig. A.3). No trend has been observed for Oquillas stand, where all trees were completely defoliated.

3.4. Latewood percentage

LW width was reduced during PPM (0.12 ± 0.01 mm) and drought events (0.14 ± 0.01 mm), in comparison to the rest of the years (0.31 ± 0.01 mm). EW width was lower during PPM events (0.29 ± 0.04 mm) than during drought events (0.79 ± 0.06 mm) and the rest of the years (1.57 ± 0.04 mm). Nevertheless, the most relevant difference between PPM and drought events appeared when the relative contribution of EW and LW was considered. %LW in tree ring width during PPM events (40.4% ± 3.0%) was more than twice than in drought events (20.7% ± 0.9%) or the rest of the years (17.7% ± 0.3%) (Fig. A.4). This pattern was confirmed by LMM model ($P < 0.001$; Table 2; Table A.4).

3.5. Intrinsic water-use efficiency

iWUE temporal changes showed a conspicuous decrease during PPM events, while it augmented during drought years. When BAI and iWUE temporal changes were plotted together (Fig. 4), PPM events showed a unique combination of low growth and low iWUE temporal changes, being easily distinguishable from the other events (Fig. A.5). The type of event (PPM or drought events) was extremely determinant for iWUE temporal changes values, explaining almost half of the variance of the statistical models ($P < 0.001$; Table 2; Table A.5).

3.6. Blue intensity

Minimum BI of PPM and drought events had similar averages (0.52 ± 0.02 and 0.52 ± 0.01, respectively) but was lower than the rest of the years (0.58 ± 0.00) (Fig. A.6) Accordingly, we did not find significant differences between both events ($P = 0.882$; Table 2; Table A.6).

4. Discussion

PPM and drought events cause severe reductions in tree secondary growth. Fortunately, when these events are not concurrent, they lead to distinct signatures in tree ring traits (Table 2). PPM events were characterized by higher growth variance, negative residuals in climate growth models, tree rings with higher %LW and lower iWUE. However, in contrast to our hypothesis, minimum BI did not differ between PPM and drought events. The combination of some of these traits enables the development of a relatively flexible framework for reconstructing PPM defoliations.

PPM events showed a lower tree growth synchrony than droughts at the stand level, as it was reflected in the higher variance of BAI (Fig. 2). Tree vulnerability to PPM is not homogeneous in space (Azcárate et al., 2023). PPM female moth exhibits limited flying ability and actively selects isolated and sun-exposed trees (Régolini et al., 2014). This biological behaviour is manifest in our data, showing decreasing defoliations across an edge-to-core gradient (Fig. 4). On the contrary, drought is a wide-scale disturbance and affects all trees, increasing growth synchrony among trees (Klisz et al., 2019). In extremely severe

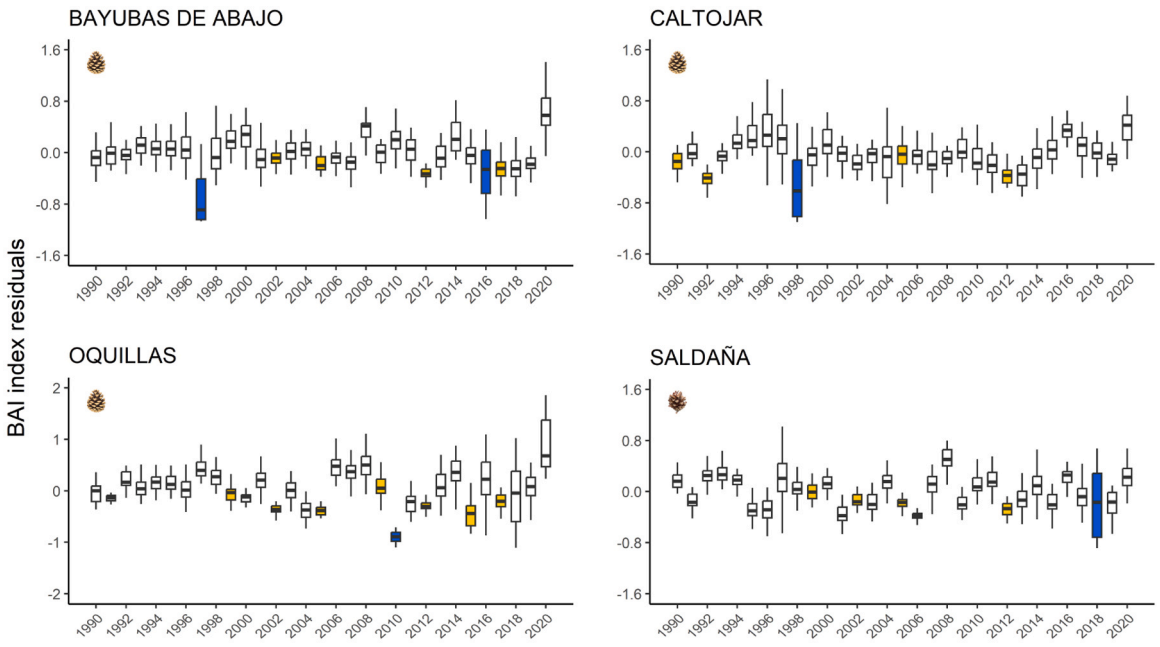

Fig. 3. Residuals of the climate growth model models over the period 1990–2020 for Bayubas (*P. nigra*; n=34), Caltojar (*P. nigra*; n=32), Oquillas (*P. nigra*; n=29) and Saldaña (*P. sylvestris*; n=37) stands. PPM and drought events are highlighted in blue and yellow, respectively. Boxplots vertical bars indicate the inter-quartile range.

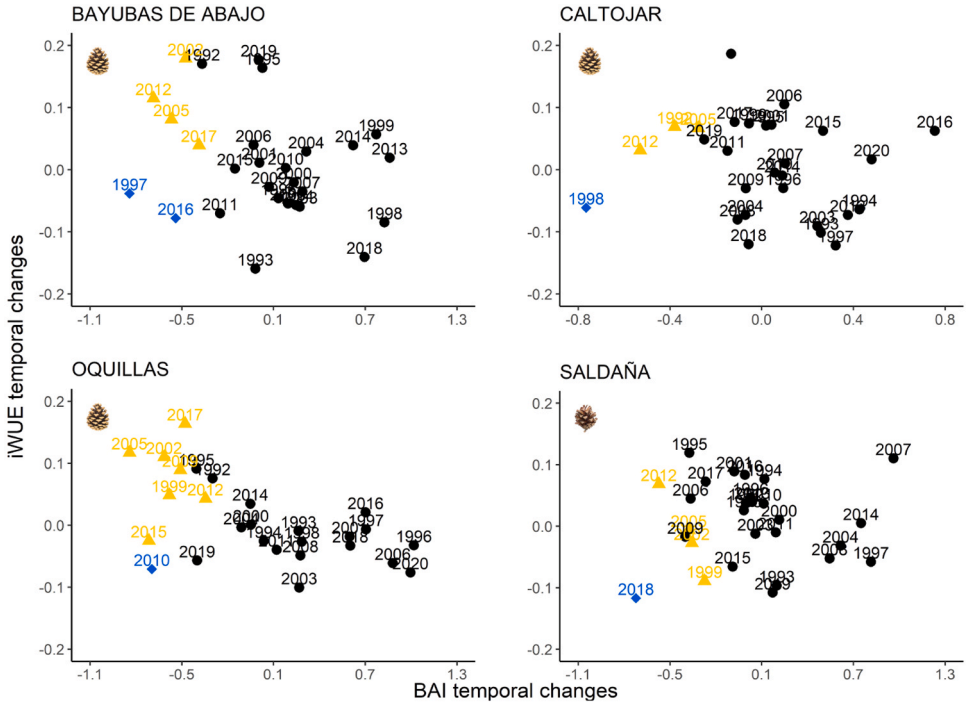

Fig. 4. Relationship between basal area increment (BAI) and intrinsic water-use efficiency (iWUE) temporal changes for Bayubas (*P. nigra;* n=5), Caltojar (*P. nigra;* n=5), Oquillas (*P. nigra;* n=5) and Saldaña stands (*P. sylvestris;* n=5) over the period 1990–2020. PPM and drought events are highlighted in blue and yellow, respectively.

PPM outbreaks, where all trees show complete defoliation, growth synchrony can be very high and growth variance low. In such case, the comparison of tree growth with nearby pine populations could provide valuable insights, and in all cases, other proxies must be considered.

PPM events induced negative climate growth residuals (Fig. 3). Drought events also resulted in negative (but higher) residuals indicating that climate growth models underestimated their effects. Droughts longer than the time scales considered in the LMMs led to lower-than-expected growth rates. A similar approach has been previously used to identify PPM defoliations (Sangüesa-Barreda et al., 2014), as well as other biotic disturbances, such as larch budmoth defoliation (Kunz et al., 2023) or mistletoe infestations (Camarero et al., 2019). Overall, the combination of synchrony and climate growth residuals has a strong potential for identifying PPM outbreaks. Nevertheless, the use

of climate growth model residuals is limited to periods with instrumental records.

PPM events affected the relative contribution of EW and LW to tree ring. LW showed a higher contribution to total ring width during PPM events than in drought events. In Mediterranean habitats, drought usually intensifies as growing season advances, impacting on cell division rate with more intensity in the last part of the ring (Olano et al., 2012). In contrast, PPM defoliation in winter limits carbon acquisition at the onset of the growing season and induces the remobilization of carbon to canopy formation, thus limiting temporally the secondary growth (Palacio et al., 2012). Consequently, this results in a reduction or a total loss of the relative contribution of EW. Such diminution in EW production had also been reported in conifers affected by other winter moth defoliators (Simmons et al., 2014), whereas when insect defoliations occur after EW formation, only LW growth is affected (Axelson et al., 2014).

PPM and drought events had disparate effects on iWUE (Fig. 4). Drought increased iWUE (Martin-Benito et al., 2017; Olano et al., 2014; Peters et al., 2018). Drought drives stomatal closure to prevent water loss, thereby limiting CO_2 availability in the substomatal chamber (Levesque et al., 2017), leading to a ^{13}C enrichment of fixed carbon. In contrast, PPM defoliations were associated to a decrease in iWUE. This result differs with previous studies that showed either no defoliation effect on iWUE (McIntire et al., 2021), or even an increase in iWUE (Simard et al., 2008), but it is in line of a recent observation relative to a detailed analysis of a PPM event (Camarero et al., 2023). Canopy loss decreases leaf to sapwood area ratio, increasing sap flow per leaf area and, therefore, reduces water constraint and stomatal closure, leading to lower iWUE (Mencuccini and Grace, 1995). A complementary mechanism is linked to the effect of defoliation in carbon dynamics canopy. Defoliation implies simultaneously a sharp loss of carbon gain and a high cost to build a new canopy, with this process being particularly costly in perennial plants with high leaf construction costs (Poorter et al., 2009). To cope with these demands, plants usually remobilize older carbohydrates stored in stem to sustain growth recovery (D'Andrea et al., 2019; Herrera-Ramírez et al., 2020). Since iWUE is increasing gradually due to higher atmospheric CO_2 concentrations (Olano et al., 2014; Olano et al., 2023), older carbohydrates would show lower iWUE. If this was the dominant mechanism driving the decrease in iWUE, this promising proxy to discriminate drought and PPM events could not be applied to preindustrial periods.

Finally, PPM events had lower minimum BI (Esper et al., 2007), but this trait did not discriminate between drought and PPM events. Low density in PPM events is attributable to a reduction in available carbohydrates and the construction of lighter tree rings (Hogg et al., 2002). Drought also presented a lower minimum BI, however, such effect does not necessarily imply a reduction in available carbon, since photosynthetic activity (source activity) is more tolerant to drought stress than xylogenesis (sink activity) (Körner, 2003). Thus, factors limiting xylogenetic activity may result in less lignified rings, as it has been repeatedly reported in relation to temperature (Björklund et al., 2014; Martin-Benito et al., 2017; Seftigen et al., 2020).

5. Conclusions

The reconstruction of PPM events is a challenge in Mediterranean environments where narrow rings associated to droughts are very common. Our study highlights the existence of a panoply of tree ring traits to discriminate both disturbances. The combination of climate growth residuals, growth synchrony and latewood percentage has a strong potential with the advantage that it can be run using just basic ring width measurements and has limited costs. However, moving towards preinstrumental periods implies the loss of climate growth residuals. iWUE robustly discerns between PPM (low efficiency) and drought (high efficiency) events, but further research must be done to assess that the mechanism driving low iWUE values in PPM events is not affected by historical changes in CO_2. In contrast, the differences in the relative contribution of EW and LW to final ring width seems supported by biological mechanisms that are stable in time. These findings provide a new avenue for the reconstruction of PPM incidence over hundreds of years, and the examination of the PPM impact in relation to the long-term rising temperature trend.

CRediT authorship contribution statement

Darío Domingo: Writing – review & editing, Formal analysis, Data curation. **Antonio Delgado-Huertas:** Resources, Formal analysis. **Miguel García-Hidalgo:** Writing – review & editing, Resources, Methodology, Conceptualization. **Gabriel Sangüesa-Barreda:** Writing – review & editing, Writing – original draft, Validation, Supervision, Project administration, Methodology, Investigation, Funding acquisition, Formal analysis, Data curation, Conceptualization. **Héctor Hernández-Alonso:** Writing – review & editing, Validation, Methodology, Data curation, Conceptualization. **Cristina Gómez:** Writing – review & editing, Validation, Formal analysis, Data curation. **Hermine Houdas:** Writing – review & editing, Writing – original draft, Methodology, Investigation, Formal analysis, Data curation. **José Miguel Olano:** Writing – review & editing, Writing – original draft, Validation, Supervision, Methodology, Funding acquisition, Conceptualization.

Declaration of Competing Interest

The authors declare that they have no known competing financial interests or personal relationships that could have appeared to influence the work reported in this paper.

Data availability

The data that has been used is confidential.

Acknowledgements

We thank to the Junta de Castilla y León for providing sampling permissions and sharing their data from its pest monitoring program. This work is part of the PROWARM project (PID2020–118444GA-I00) funded by Ministerio de Ciencia, Innovación y Universidades, y Agencia Estatal de Investigación MICIU/ AEI /10.13039/501100011033, and OUTBREAK project (VA171P20) funded by Junta de Castilla y León and UE Feder Funds. HH was supported by a predoctoral contract (PRE2021–098278) funded by MICIU/ AEI /10.13039/501100011033 and ESF Investing in your future, GSB was supported by a postdoctoral grant (IJC2019–040571-I) funded by MICIU/ AEI /10.13039/501100011033, and DD was supported by European Union-NextGeneration EU Margarita Salas contract (MS-240621).

Appendix A

.

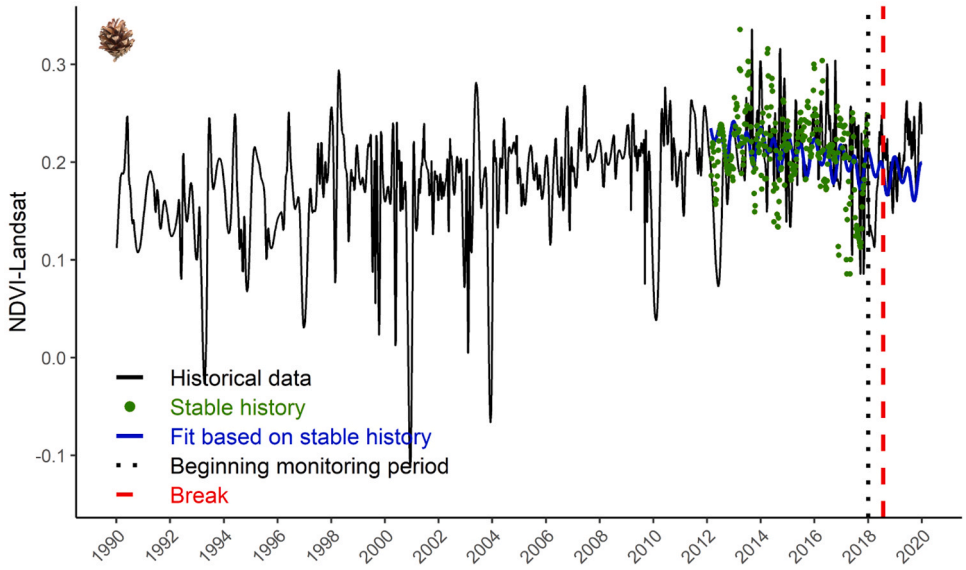

Figure A.1. LANDSAT-NDVI time series over the period 1990–2020 of Saldaña stand (*P. sylvestris*). The period from 2012 until 2018 constituted the stable period used by *bfastmonitor* to assess data variation patterns (blue line) and thus enable disturbance detection. Here, a break from the LANDSAT-NDVI time series patterns was detected in 2018.

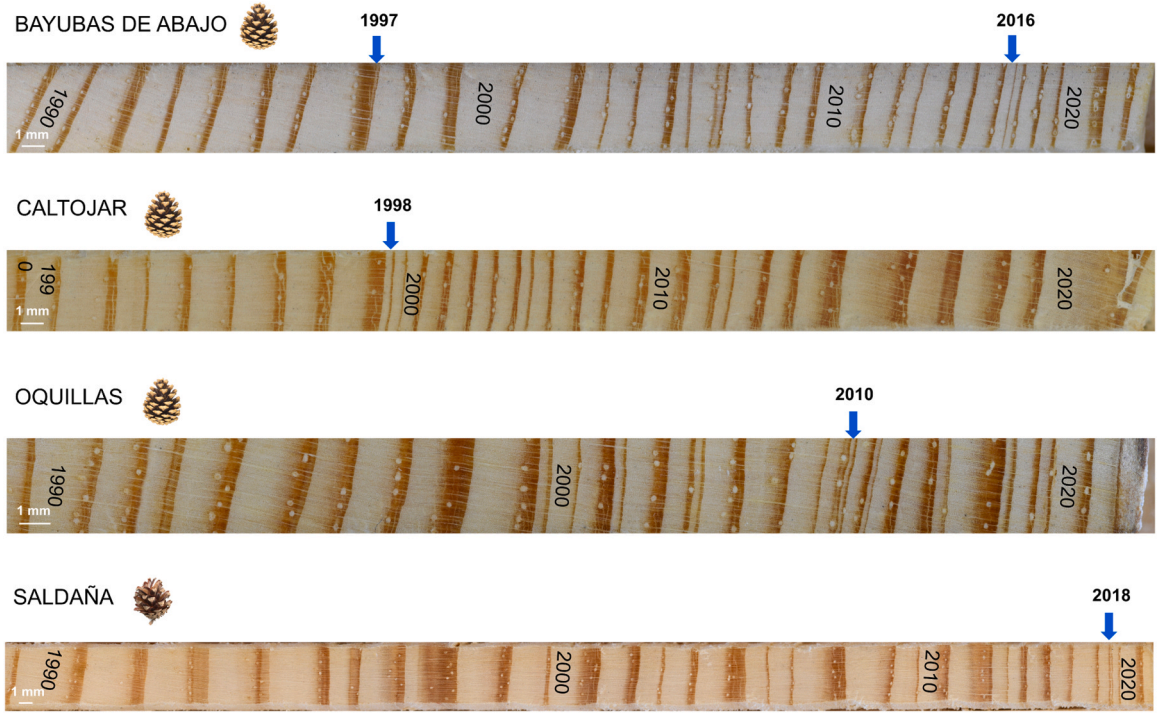

Figure A.2. Images of tree rings and years of PPM outbreaks in Bayubas (*P. nigra*), Caltojar, (*P. nigra*), Oquillas (*P. nigra*) and Saldaña (*P. sylvestris)* stands.

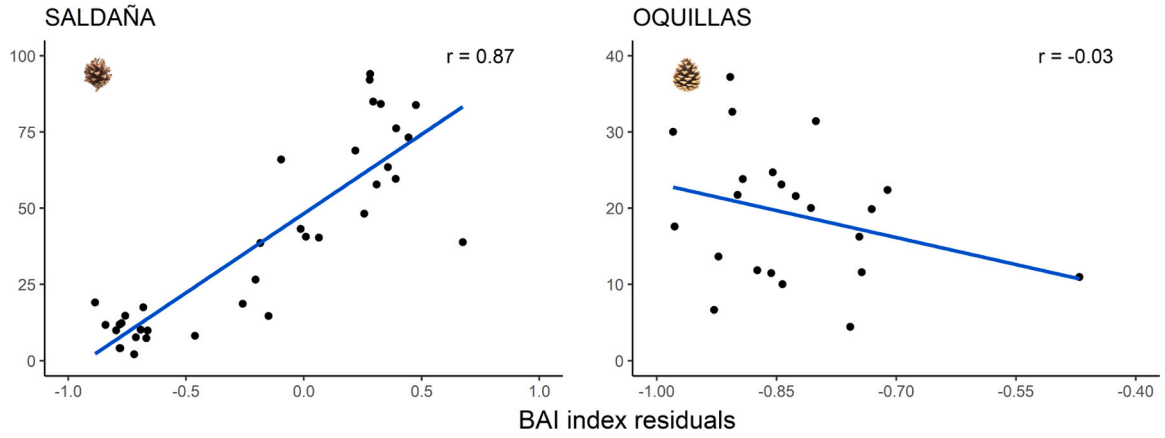

Figure A.3. Linear relationship between residuals of climate growth models during PPM events and tree distance to the edge in Saldaña (*P. sylvestris*; n=37) and Oquillas (*P. nigra*; n=29) stands. Pearson's correlation coefficient (r) is also indicated.

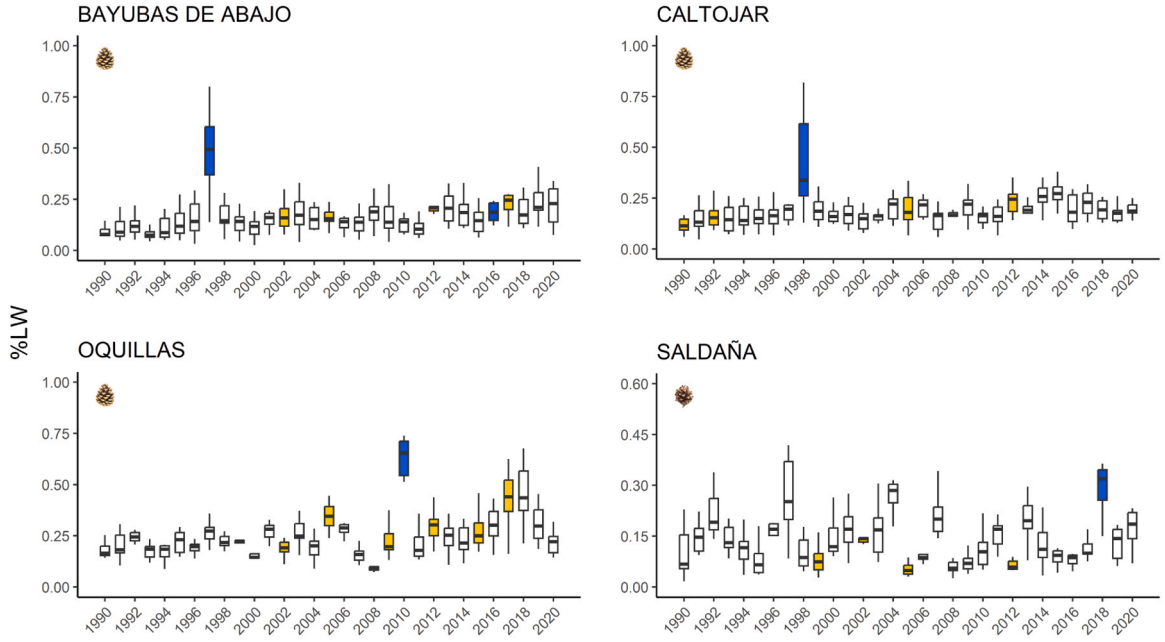

Figure A.4. %LW of tree rings over the period 1990–2020 for Bayubas (*P. nigra*; n=10), Caltojar (*P. nigra*; n=10), Oquillas (*P. nigra*; n=10) and Saldaña (*P. sylvestris*; n=10) stands. PPM and drought events are highlighted in blue and yellow, respectively. Boxplots vertical bars indicate the interquartile range.

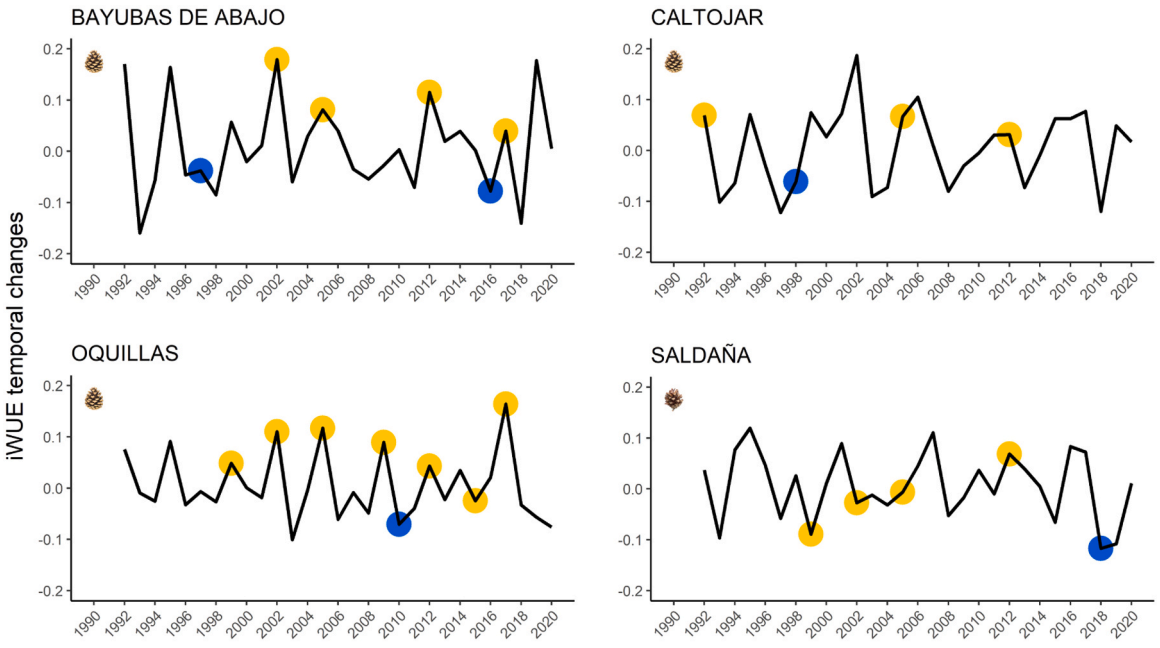

Figure A.5. Mean iWUE temporal changes of the trees over the period 1990–2020 for Bayubas (*P. nigra*; n=5), Caltojar (*P. nigra*; n=5), Oquillas (*P. nigra*; n=5) and Saldaña (*P. sylvestris*; n=5) stands. PPM and drought events with blue and yellow dots, respectively.

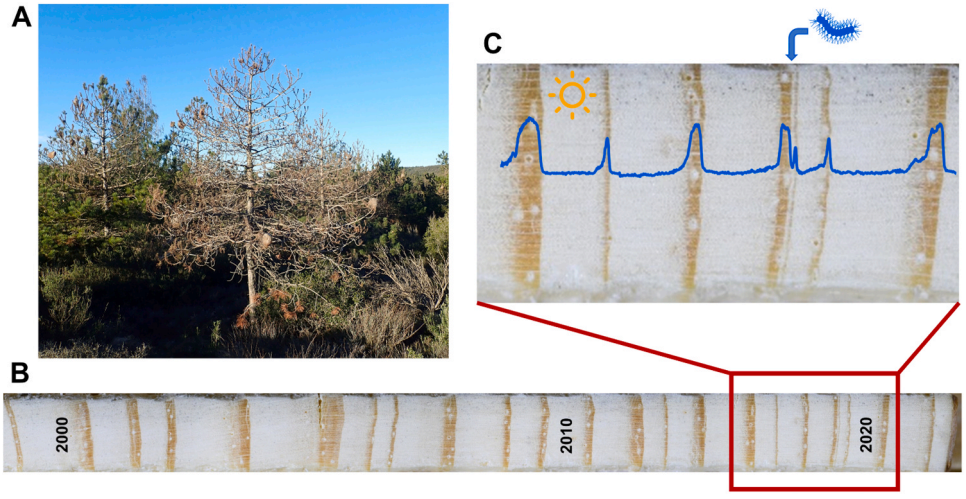

Figure A.6. A) Effect of PPM defoliations on the pine tree canopy, B) on radial growth, C) and detailed image with inverted minimum BI profile (for parallelism with wood density). Minimum BI value for latewood in 2018 is reduced in comparison to non PPM years.

Table A.1
PPM and drought events identified, and period with largest SPEI signal for each stand used in climate growth models.

Site	PPM events	Drought events	SPEI and lag
Bayubas	1997, 2016	2002, 2005, 2012, 2017	April SPEI 8 (r=0.50)
Caltojar	1998	1990, 1992, 2005, 2012	July SPEI 11 (r=0.43)
Oquillas	2010	1999, 2002, 2005, 2009, 2012, 2015, 2017	May SPEI 11 (r=0.52)
Saldaña	2018	1999, 2002, 2005, 2012	January SPEI 5 (r=0.28)

Table A.2
Summary of parameters and estimators of the linear mixed model (LMM) used to assess the effect of the type of event (PPM event/drought event) on basal area increment (BAI) variance. SE stands for standard error. $P < 0.05$ in bold.

Growth variance			
Predictors	**Estimates**	**SE**	***P***

(*continued on next page*)

Table A.2 (*continued*)

Growth variance			
Predictors	**Estimates**	**SE**	***P***
(Intercept)	0.05	0.02	**0.039**
Event	0.12	0.05	**0.023**
Observations			24
Marginal R^2			0.210
Conditional R^2			0.210

Table A.3
Summary of parameters and estimators of linear mixed model (LMM) used to assess the effect of the type of event (PPM event/drought event) on the residuals of the climate growth models. SE stands for standard error. $P < 0.05$ in bold.

Residuals of climate growth models			
Predictors	**Estimates**	**SE**	***P***
(Intercept)	-0.20	0.01	**<0.001**
Event	-0.30	0.03	**<0.001**
Observations			780
Marginal R^2			0.133
Conditional R^2			0.155

Table A.4
Summary of parameters and estimators of the generalized linear mixed model (GLMM) used to assess the effect of the type of event (PPM event/drought event) on the percentage of latewood (%LW). SE stands for standard error. $P < 0.05$ in bold.

%LW			
Predictors	**Estimates**	**SE**	***P***
(Intercept)	-3.61	0.45	**<0.001**
Event	2.94	0.54	**<0.001**
Observations			239
Marginal R^2			0.304
Conditional R^2			0.304

Table A.5
Summary of parameters and estimators of the linear mixed model (LMM) used to assess the effect of the type of event (PPM event/drought event) on intrinsic water-use efficiency (iWUE) temporal changes. SE stands for standard error. $P < 0.05$ in bold.

iWUE temporal changes			
Predictors	**Estimates**	**SE**	***P***
(Intercept)	0.06	0.02	**0.023**
Event	-0.14	0.03	**<0.001**
Observations			23
Marginal R^2			0.437
Conditional R^2			0.633

Table A.6
Summary of parameters and estimators of the linear mixed model (LMM) used to assess the effect of the type of event (PPM event/drought event) on minimum BI. SE stands for standard error. $P < 0.05$ in bold.

Minimum BI			
Predictors	**Estimates**	**SE**	***P***
(Intercept)	0.52	0.01	**<0.001**
Event	0.00	0.01	0.882
Observations			253
Marginal R^2			0.000
Conditional R^2			0.561

References

Axelson, J.N., Bast, A., Alfaro, R., Smith, D.J., Gärtner, H., 2014. Variation in wood anatomical structure of Douglas-fir defoliated by the western spruce budworm: a case study in the coastal-transitional zone of British Columbia, Canada. Trees 28, 1837–1846. https://doi.org/10.1007/s00468-014-1091-1.

Ayres, M.P., Lombardero, M.J., 2000. Assessing the consequences of global change for forest disturbance from herbivores and pathogens. Sci. Total Environ. 262, 263–286. https://doi.org/10.1016/S0048-9697(00)00528-3.

Azcárate, F.M., Seoane, J., Silvestre, M., 2023. Factors affecting pine processionary moth (*Thaumetopoea pityocampa*) incidence in Mediterranean pine stands: a multiscale approach. . Ecol. Manag. 529, 120728 https://doi.org/10.1016/j.foreco.2022.120728.

Barbaro, L., Battisti, A., 2011. Birds as predators of the pine processionary moth (Lepidoptera: Notodontidae). Biol. Control. 56, 107–114. https://doi.org/10.1016/j.biocontrol.2010.10.009.

Battisti, A., Stastny, M., Buffo, E., Larsson, S., 2006. A rapid altitudinal range expansion in the pine processionary moth produced by the 2003 climatic anomaly. Glob. Chang. Biol. 12, 662–671. https://doi.org/10.1111/j.1365-2486.2006.01124.x.

Battisti, A., Stastny, M., Netherer, S., Robinet, C., Schopf, A., Roques, A., Larsson, S., 2005. Expansion of the geographic range in the pine processionary moth caused by increased winter temperatures. Ecol. Appl. 15, 2084–2096. https://doi.org/10.1890/04-1903.

Biondi, F., Qeadan, F., 2008. A theory-driven approach to tree ring standardization: defining the biological trend from expected basal area increment. Tree Ring Res 64, 81–96. https://doi.org/10.3959/2008-6.1.

Björklund, J.A., Gunnarson, B.E., Seftigen, K., Esper, J., Linderholm, H.W., 2014. Blue intensity and density from northern Fennoscandian tree rings, exploring the potential to improve summer temperature reconstructions with earlywood information. Clim 10, 877–885. https://doi.org/10.5194/cp-10-877-2014.

Briffa, K.R., Osborn, T.J., Schweingruber, F.H., Jones, P.D., Shiyatov, S.G., Vaganov, E. A., 2002. Tree ring width and density data around the Northern Hemisphere: Part 1, local and regional climate signals. Holocene 12, 737–757. https://doi.org/10.1191/0959683602hl587rp.

Buffo, E., Battisti, A., Stastny, M., Larsson, S., 2007. Temperature as a predictor of survival of the pine processionary moth in the Italian Alps. Agric. . Entomol. 9, 65–72. https://doi.org/10.1111/j.1461-9563.2006.00321.x.

Bunn, A.G., 2008. A dendrochronology program library in R (dplR). Dendrochronologia 26, 115–124. https://doi.org/10.1016/j.dendro.2008.01.002.

Camarero, J.J., Manzanedo, R.D., Sanchez-Salguero, R., Navarro-Cerrillo, R.M., 2013. Growth response to climate and drought change along an aridity gradient in the southernmost Pinus nigra relict forests. Ann. . Sci. 70, 769–780. https://doi.org/10.1007/s13595-013-0321-9.

Camarero, J.J., Tardif, J., Gazol, A., Conciatori, F., 2022. Pine processionary moth outbreaks cause longer growth legacies than drought and are linked to the North Atlantic Oscillation. Sci. Total Environ. 819, 153041 https://doi.org/10.1016/j.scitotenv.2022.153041.

Camarero, J.J., González De Andrés, E., Sangüesa-Barreda, G., Rita, A., Colangelo, M., 2019. Long- and short-term impacts of a defoliating moth plus mistletoe on tree growth, wood anatomy and water-use efficiency. Dendrochronologia 56, 125598. https://doi.org/10.1016/j.dendro.2019.05.002.

Camarero, J.J., Colangelo, M., Rita, A., Hevia, A., Pizarro, M., Voltas, J., 2023. A multi-proxy framework to detect insect defoliations in tree rings: a case study on pine processionary. Front. Ecol. Evol. 11, 1192036 https://doi.org/10.3389/fevo.2023.1192036.

D'Andrea, E., Rezaie, N., Battistelli, A., Gavrichkova, O., Kuhlmann, I., Matteucci, G., Moscatello, S., Proietti, S., Scartazza, A., Trumbore, S., Muhr, J., 2019. Winter's bite: beech trees survive complete defoliation due to spring late-frost damage by mobilizing old C reserves. N. Phytol. 224, 625–631. https://doi.org/10.1111/nph.16047.

Dale, V.H., Joyce, L.A., McNulty, S., Neilson, R.P., 2000. The interplay between climate change, forests, and disturbances. Sci. Total Environ. 262, 201–204. https://doi.org/10.1016/S0048-9697(00)00522-2.

Démolin, G., 1969. Bioecología de la procesionaria del pino *Thaumetopoea pityocampa* Schiff.: incidencia de los factores climáticos. Bol. Serv. Plagas 12, 9–24.

Dymond, C.C., Neilson, E.T., Stinson, G., Porter, K., MacLean, D.A., Gray, D.R., Campagna, M., Kurz, W.A., 2010. Future spruce budworm outbreak may create a carbon source in eastern Canadian forests. Ecosystems 13, 917–931. https://doi.org/10.1007/s10021-010-9364-z.

Esper, J., Büntgen, U., Frank, D.C., Nievergelt, D., Liebhold, A., 2007. 1200 years of regular outbreaks in alpine insects. Proc. R. Soc. B. 274, 671–679. https://doi.org/10.1098/rspb.2006.0191.

FAO, 2005. Global Forest Resource Assessment (FRA) 2005. License: CC BY-NC-SA 3.0 IGO, Rome. ⟨https://www.fao.org/forestry/fra/fra2005/en/⟩.

Farquhar, G., Richards, R., 1984. Isotopic composition of plant carbon correlates with water-use efficiency of wheat genotypes. Funct. Plant Biol. 11, 539. https://doi.org/10.1071/PP9840539.

Field, C.B., Raupach, M.R. (Eds.), 2004. The global carbon cycle: integrating humans, climate, and the natural world, SCOPE. Island Press, Washington.

García-Hidalgo, M., Sangüesa-Barreda, G., Houdas, H., Rozas, V., Olano, J.M., 2023. Open-Source Solutions for High-Resolution Spectral Analysis of wood using CaptuRING. Poster presented at the TRACE 2023, Coimbra.

García-Hidalgo, M., García-Pedrero, Á.M., Caetano-Sánchez, C., Gómez-España, M., Lillo-Saavedra, M., Olano, J.M., 2021. ρ-MtreeRing: a graphical user interface for X-ray microdensity analysis. Forests 12, 1405. https://doi.org/10.3390/f12101405.

García-Hidalgo, M., García-Pedrero, Á., Colón, D., Sangüesa-Barreda, G., García-Cervigón, A.I., López-Molina, J., Hernández-Alonso, H., Rozas, V., Olano, J.M., Alonso-Gómez, V., 2022. CaptuRING: a do-it-yourself tool for wood sample digitization. Methods Ecol. Evol. 13, 1185–1191. https://doi.org/10.1111/2041-210X.13847.

Gazol, A., Hernández-Alonso, R., Camarero, J.J., 2019. Patterns and drivers of pine processionary moth defoliation in Mediterranean mountain forests. Front. Ecol. Evol. 7, 458. https://doi.org/10.3389/fevo.2019.00458.

Gazol, A., Rozas, V., Cuende Arribas, S., Alonso Ponce, R., Rodríguez-Puerta, F., Gómez, C., Olano, J.M., 2023. Stand characteristics modulate secondary growth responses to drought and gross primary production in *Pinus halepensis* afforestation. Eur. J. . Res. 142, 353–366. https://doi.org/10.1007/s10342-022-01526-9.

Goward, S.N., Dye, D.G., 1987. Evaluating North American net primary productivity with satellite observations. Adv. Space Res. 7, 165–174. https://doi.org/10.1016/0273-1177(87)90308-5.

Graven, H., Allison, C.E., Etheridge, D.M., Hammer, S., Keeling, R.F., Levin, I., Meijer, H. A.J., Rubino, M., Tans, P.P., Trudinger, C.M., Vaughn, B.H., White, J.W.C., 2017. Compiled records of carbon isotopes in atmospheric CO2 for historical simulations in CMIP6. Geosci. Model Dev. 10, 4405–4417. https://doi.org/10.5194/gmd-10-4405-2017.

Harrington, R., Fleming, R.A., Woiwod, I.P., 2001. Climate change impacts on insect management and conservation in temperate regions: can they be predicted? Agric. . Entomol. 3, 233–240. https://doi.org/10.1046/j.1461-9555.2001.00120.x.

Harris, I., Osborn, T.J., Jones, P., Lister, D., 2020. Version 4 of the CRU TS monthly high-resolution gridded multivariate climate dataset. Sci. Data 7, 109. https://doi.org/10.1038/s41597-020-0453-3.

Herrera-Ramírez, D., Muhr, J., Hartmann, H., Römermann, C., Trumbore, S., Sierra, C.A., 2020. Probability distributions of nonstructural carbon ages and transit times provide insights into carbon allocation dynamics of mature trees. N. Phytol. 226, 1299–1311. https://doi.org/10.1111/nph.16461.

Hódar, J.A., Zamora, R., Castro, J., 2002. Host utilisation by moth and larval survival of pine processionary caterpillar *Thaumetopoea pityocampa* in relation to food quality in three *Pinus* species: food quality in a plant-insect interaction. Ecol. Entomol. 27, 292–301. https://doi.org/10.1046/j.1365-2311.2002.00415.x.

Hódar, J.A., Zamora, R., Cayuela, L., 2012. Climate change and the incidence of a forest pest in Mediterranean ecosystems: can the North Atlantic Oscillation be used as a predictor? Clim. Change 113, 699–711. https://doi.org/10.1007/s10584-011-0371-7.

Hogg, E.H., Hart, M., Lieffers, V.J., 2002. White tree rings formed in trembling aspen saplings following experimental defoliation. Can. J. . Res. 32, 1929–1934. https://doi.org/10.1139/x02-114.

Holmes, R.L., 1983. Computer-assisted quality control in tree ring dating and measurement. Tree Ring Bull. 43, 69–78.

Jacquet, J.S., Orazio, C., Jactel, H., 2012. Defoliation by processionary moth significantly reduces tree growth: a quantitative review. Ann. . Sci. 69, 857–866. https://doi.org/10.1007/s13595-012-0209-0.
Kaczka, R.J., Spyt, B., Janecka, K., Beil, I., Büntgen, U., Scharnweber, T., Nievergelt, D., Wilmking, M., 2018. Different maximum latewood density and blue intensity measurements techniques reveal similar results. Dendrochronologia 49, 94–101. https://doi.org/10.1016/j.dendro.2018.03.005.
Klisz, M., Puchałka, R., Wilczyński, S., Kantorowicz, W., Jabłoński, T., Kowalczyk, J., 2019. The effect of insect defoliations and seed production on the dynamics of radial growth synchrony among Scots pine *Pinus sylvestris* L. Provenances. Forests 10, 934. https://doi.org/10.3390/f10100934.
Körner, C., 2003. Carbon limitation in trees. J. Ecol. 91, 4–17. https://doi.org/10.1046/j.1365-2745.2003.00742.x.
Kriticos, D.J., Leriche, A., Palmer, D.J., Cook, D.C., Brockerhoff, E.G., Stephens, A.E.A., Watt, M.S., 2013. Linking climate suitability, spread rates and host-impact when estimating the potential costs of invasive pests. PLoS ONE 8, e54861. https://doi.org/10.1371/journal.pone.0054861.
Kunz, M., Esper, J., Kuhl, E., Schneider, L., Büntgen, U., Hartl, C., 2023. Combining tree ring width and density to separate the effects of climate variation and insect defoliation. Forests 14, 1478. https://doi.org/10.3390/f14071478.
Kurz, W.A., Dymond, C.C., Stinson, G., Rampley, G.J., Neilson, E.T., Carroll, A.L., Ebata, T., Safranyik, L., 2008. Mountain pine beetle and forest carbon feedback to climate change. Nature 452, 987–990. https://doi.org/10.1038/nature06777.
Laurent, L., Mårell, A., Korboulewsky, N., Saïd, S., Balandier, P., 2017. How does disturbance affect the intensity and importance of plant competition along resource gradients? . Ecol. Manag. 391, 239–245. https://doi.org/10.1016/j.foreco.2017.02.003.
Levesque, M., Andreu-Hayles, L., Pederson, N., 2017. Water availability drives gas exchange and growth of trees in northeastern US, not elevated CO_2 and reduced acid deposition. Sci. Rep. 7, 46158 https://doi.org/10.1038/srep46158.
Lucas-Borja, M.E., Andivia, E., Candel-Pérez, D., Linares, J.C., Camarero, J.J., 2021. Long term forest management drives drought resilience in Mediterranean black pine forest. Trees 35, 1651–1662. https://doi.org/10.1007/s00468-021-02143-6.
Lynch, A.M., 2012. What tree ring reconstruction tells us about conifer defoliator outbreaks. In: Barbosa, P., Letourneau, D.K., Agrawal, A.A. (Eds.), Insect Outbreaks Revisited. Wiley, pp. 126–154. https://doi.org/10.1002/9781118295205.ch7.
Martin-Benito, D., Anchukaitis, K., Evans, M., Del Río, M., Beeckman, H., Cañellas, I., 2017. Effects of drought on xylem anatomy and water-use efficiency of two co-occurring Pine Species. Forests 8, 332. https://doi.org/10.3390/f8090332.
McCarroll, D., Loader, N.J., 2004. Stable isotopes in tree rings. Quat. Sci. Rev. 23, 771–801. https://doi.org/10.1016/j.quascirev.2003.06.017.
McCarroll, D., Pettigrew, E., Luckman, A., Guibal, F., Edouard, J.-L., 2002. Blue reflectance provides a surrogate for latewood density of high-latitude pine tree rings. Arct. Antarct. Alp. Res. 34, 450–453. https://doi.org/10.1080/15230430.2002.12003516.
McIntire, C.D., Huggett, B.A., Dunn, E., Munck, I.A., Vadeboncoeur, M.A., Asbjornsen, H., 2021. Pathogen-induced defoliation impacts on transpiration, leaf gas exchange, and non-structural carbohydrate allocation in eastern white pine (*Pinus strobus*). Trees 35, 357–373. https://doi.org/10.1007/s00468-020-02037-z.
Mencuccini, M., Grace, J., 1995. Climate influences the leaf area/sapwood area ratio in Scots pine. Tree Physiol. 15, 1–10. https://doi.org/10.1093/treephys/15.1.1.
Netherer, S., Schopf, A., 2010. Potential effects of climate change on insect herbivores in European forests—General aspects and the pine processionary moth as specific example. . Ecol. Manag. 259, 831–838. https://doi.org/10.1016/j.foreco.2009.07.034.
Olano, J.M., Eugenio, M., García-Cervigón, A.I., Folch, M., Rozas, V., 2012. Quantitative tracheid anatomy reveals a complex environmental control of wood structure in continental Mediterranean climate. Int. J. Plant Sci. 173, 137–149. https://doi.org/10.1086/663165.
Olano, J.M., Linares, J.C., García-Cervigón, A.I., Arzac, A., Delgado, A., Rozas, V., 2014. Drought-induced increase in water-use efficiency reduces secondary tree growth and tracheid wall thickness in a Mediterranean conifer. Oecologia 176, 273–283. https://doi.org/10.1007/s00442-014-2989-4.
Olano, J.M., Sangüesa-Barreda, G., García-López, M.A., García-Hidalgo, M., Rozas, V., García-Cervigón, A.I., Delgado-Huertas, A., Hernández-Alonso, H., 2023. Water use efficiency and climate legacies dominate beech growth at its rear edge. J. Ecol. 111, 2160–2171. https://doi.org/10.1111/1365-2745.14164.
Otsu, K., Pla, M., Vayreda, J., Brotons, L., 2018. Calibrating the severity of forest defoliation by pine processionary moth with Landsat and UAV imagery. Sensors 18, 3278. https://doi.org/10.3390/s18103278.
Palacio, S., Hernández, R., Maestro-Martínez, M., Camarero, J.J., 2012. Fast replenishment of initial carbon stores after defoliation by the pine processionary moth and its relationship to the re-growth ability of trees. Trees 26, 1627–1640. https://doi.org/10.1007/s00468-012-0739-y.
Pan, Y., Chen, J.M., Birdsey, R., McCullough, K., He, L., Deng, F., 2011. Age structure and disturbance legacy of North American forests. Biogeosciences 8, 715–732. https://doi.org/10.5194/bg-8-715-2011.
Pasho, E., Camarero, J.J., De Luis, M., Vicente-Serrano, S.M., 2011. Impacts of drought at different time scales on forest growth across a wide climatic gradient in north-eastern Spain. Agric. . Meteorol. 151, 1800–1811. https://doi.org/10.1016/j.agrformet.2011.07.018.
Peters, W., Van Der Velde, I.R., Van Schaik, E., Miller, J.B., Ciais, P., Duarte, H.F., Van Der Laan-Luijkx, I.T., Van Der Molen, M.K., Scholze, M., Schaefer, K., Vidale, P.L., Verhoef, A., Wårlind, D., Zhu, D., Tans, P.P., Vaughn, B., White, J.W.C., 2018. Increased water-use efficiency and reduced CO_2 uptake by plants during droughts at a continental scale. Nat. Geosci. 11, 744–748. https://doi.org/10.1038/s41561-018-0212-7.
Pinheiro, J., Bates, D., R Core Team, 2023. nlme: Linear and Nonlinear Mixed Effects Models. R package version 3.1-163, ⟨https://CRAN.R-project.org/package=nlme⟩.
Polge, H., 1970. The use of X-ray densitometric methods in dendrochronology. Tree ring Bull. 30, 1–10. ⟨http://hdl.handle.net/10150/259942⟩.
Poorter, H., Niinemets, Ü., Poorter, L., Wright, I.J., Villar, R., 2009. Causes and consequences of variation in leaf mass per area (LMA): a meta-analysis. N. Phytol. 182, 565–588. https://doi.org/10.1111/j.1469-8137.2009.02830.x.
QGIS Development Team, 2023. QGIS Geographic Information System. Open Source Geospatial Foundation Project. ⟨http://qgis.osgeo.org⟩.
R Core Team, 2023. R: A Language and Environment for Statistical Computing. R Foundation for Statistical Computing, Vienna. ⟨https://www.R-project.org/⟩.
Ramsfield, T.D., Bentz, B.J., Faccoli, M., Jactel, H., Brockerhoff, E.G., 2016. Forest health in a changing world: effects of globalization and climate change on forest insect and pathogen impacts. Forestry 89, 245–252. https://doi.org/10.1093/forestry/cpw018.
Régolini, M., Castagneyrol, B., Dulaurent-Mercadal, A.-M., Piou, D., Samalens, J.-C., Jactel, H., 2014. Effect of host tree density and apparency on the probability of attack by the pine processionary moth. . Ecol. Manag. 334, 185–192. https://doi.org/10.1016/j.foreco.2014.08.038.
Robinet, C., Roques, A., 2010. Direct impacts of recent climate warming on insect populations. Integr. Zool. 5, 132–142. https://doi.org/10.1111/j.1749-4877.2010.00196.x.
Roques, A., Rousselet, J., Avcı, M., Avtzis, D.N., Basso, A., Battisti, A., Ben Jamaa, M.L., Bensidi, A., Berardi, L., Berretima, W., Branco, M., Chakali, G., Çota, E., Dautbašić, M., Delb, H., El Alaoui El Fels, M.A., El Mercht, S., El Mokhefi, M., Forster, B., Garcia, J., Georgiev, G., Glavendekić, M.M., Goussard, F., Halbig, P., Henke, L., Hernańdez, R., Hódar, J.A., İpekdal, K., Jurc, M., Klimetzek, D., Laparie, M., Larsson, S., Mateus, E., Matošević, D., Meier, F., Mendel, Z., Meurisse, N., Mihajlović, L., Mirchev, P., Nasceski, S., Nussbaumer, C., Paiva, M.-R., Papazova, I., Pino, J., Podlesnik, J., Poirot, J., Protasov, A., Rahim, N., Sańchez Peña, G., Santos, H., Sauvard, D., Schopf, A., Simonato, M., Tsankov, G., Wagenhoff, E., Yart, A., Zamora, R., Zamoum, M., Robinet, C., 2015. Climate warming and past and present distribution of the processionary moths (*Thaumetopoea* spp.) in Europe, Asia Minor and North Africa. In: Roques, A. (Ed.), Processionary Moths and Climate Change: An Update. Springer Netherlands, Dordrecht, pp. 81–161. https://doi.org/10.1007/978-94-017-9340-7_3.
Rydval, M., Larsson, L.-Å., McGlynn, L., Gunnarson, B.E., Loader, N.J., Young, G.H.F., Wilson, R., 2014. Blue intensity for dendroclimatology: Should we have the blues? Experiments from Scotland. Dendrochronologia 32, 191–204. https://doi.org/10.1016/j.dendro.2014.04.003.
Sangüesa-Barreda, G., Camarero, J.J., García-Martín, A., Hernández, R., de la Riva, J., 2014. Remote-sensing and tree-ring based characterization of forest defoliation and growth loss due to the Mediterranean pine processionary moth. . Ecol. Manag. 320, 171–181. https://doi.org/10.1016/j.foreco.2014.03.008.
Sangüesa-Barreda, G., Camarero, J.J., Sánchez-Salguero, R., Gutiérrez, E., Linares, J.C., Génova, M., Ribas, M., Tíscar, P.A., López-Sáez, J.A., 2019. Droughts and climate warming desynchronize Black pine growth across the Mediterranean Basin. Sci. Total Environ. 697, 133989 https://doi.org/10.1016/j.scitotenv.2019.133989.
Schweingruber, F.H., Eckstein, D., Serre-Bachet, F., Bräker, O.U., 1990. Identification, presentation and interpretation of event years and pointer years in dendrochronology. Dendrochronologia 8, 9–38.
Seftigen, K., Fuentes, M., Ljungqvist, F.C., Björklund, J., 2020. Using Blue Intensity from drought-sensitive *Pinus sylvestris* in Fennoscandia to improve reconstruction of past hydroclimate variability. Clim. Dyn. 55, 579–594. https://doi.org/10.1007/s00382-020-05287-2.
Senf, C., Seidl, R., Hostert, P., 2017. Remote sensing of forest insect disturbances: Current state and future directions. Int. J. Appl. Earth Obs. Geoinf. 60, 49–60. https://doi.org/10.1016/j.jag.2017.04.004.
Shestakova, T.A., Gutiérrez, E., Kirdyanov, A.V., Camarero, J.J., Génova, M., Knorre, A. A., Linares, J.C., Resco De Dios, V., Sánchez-Salguero, R., Voltas, J., 2016. Forests synchronize their growth in contrasting Eurasian regions in response to climate warming. Proc. Natl. Acad. Sci. U. S. A. 113, 662–667. https://doi.org/10.1073/pnas.1514717113.
Simard, S., Elhani, S., Morin, H., Krause, C., Cherubini, P., 2008. Carbon and oxygen stable isotopes from tree rings to identify spruce budworm outbreaks in the boreal forest of Québec. Chem. Geol. 252, 80–87. https://doi.org/10.1016/j.chemgeo.2008.01.018.
Simmons, M., Lee, T., Ducey, M., Elkinton, J., Boettner, G., Dodds, K., 2014. Effects of invasive winter moth defoliation on tree radial growth in eastern Massachusetts, USA. Insects 5, 301–318. https://doi.org/10.3390/insects5020301.
Stastny, M., Battisti, A., Petrucco-Toffolo, E., Schlyter, F., Larsson, S., 2006. Host-plant use in the range expansion of the pine processionary moth, *Thaumetopoea pityocampa*. Ecol. Entomol. 31, 481–490. https://doi.org/10.1111/j.1365-2311.2006.00807.x.
Van Der Maaten-Theunissen, M., Van Der Maaten, E., Bouriaud, O., 2015. pointRes: An R package to analyze pointer years and components of resilience. Dendrochronologia 35, 34–38. https://doi.org/10.1016/j.dendro.2015.0i5.006.
Verbesselt, J., Hyndman, R., Newnham, G., Culvenor, D., 2010. Detecting trend and seasonal changes in satellite image time series. Remote Sens. Environ. 114, 106–115. https://doi.org/10.1016/j.rse.2009.08.014.
Vicente-Serrano, S.M., Beguería, S., López-Moreno, J.I., 2010. A multiscalar drought index sensitive to global warming: The Standardized Precipitation Evapotranspiration Index. J. Clim. 23, 1696–1718. https://doi.org/10.1175/2009JCLI2909.1.

Vicente-Serrano, S.M., Camarero, J.J., Olano, J.M., Martín-Hernández, N., Peña-Gallardo, M., Tomás-Burguera, M., Gazol, A., Azorin-Molina, C., Bhuyan, U., El Kenawy, A., 2016. Diverse relationships between forest growth and the Normalized Difference Vegetation Index at a global scale. Remote Sens. Environ. 187, 14–29. https://doi.org/10.1016/j.rse.2016.10.001.

Volney, W.J.A., Fleming, R.A., 2000. Climate change and impacts of boreal forest insects. Agric. Ecosyst. Environ. 82, 283–294. https://doi.org/10.1016/S0167-8809(00)00232-2.

Wang, Q., Zeng, J., Qi, J., Zhang, X., Zeng, Y., Shui, W., Xu, Z., Zhang, R., Wu, X., Cong, J., 2021. A multi-scale daily SPEI dataset for drought characterization at observation stations over mainland China from 1961 to 2018. Earth Syst. Sci. Data 13, 331–341. https://doi.org/10.5194/essd-13-331-2021.

Wilson, R.J., Fox, R., 2021. Insect responses to global change offer signposts for biodiversity and conservation. Ecol. Entomol. 46, 699–717. https://doi.org/10.1111/een.12970.

Zuur, A.F., Ieno, E.N., Walker, N., Saveliev, A.A., Smith, G.M., 2009. Mixed effects models and extensions in ecology with R, Statistics for Biology and Health. Springer New York, New York, NY. https://doi.org/10.1007/978-0-387-87458-6.